International Journal of
Plant Biology

MDPI

Article

Comparative Transcriptome Analysis Reveals Genes Associated with Alkaloid Diversity in Javanese Long Pepper (*Piper retrofractum*) Fruits

Methat Meechuen [1], Lalita Pimsawang [2,3], Tanapon Chaisan [4], Sompid Samipak [1], Wanchai Pluempanupat [2,3,*] and Piyada Juntawong [1,5,*]

[1] Department of Genetics, Faculty of Science, Kasetsart University, Bangkok 10900, Thailand; methat.me@ku.th (M.M.); sompid.s@ku.th (S.S.)
[2] Department of Chemistry, Faculty of Science, Kasetsart University, Bangkok 10900, Thailand; lalita.pims@ku.th
[3] Center of Excellence for Innovation in Chemistry, Special Research Unit for Advanced Magnetic Resonance, Faculty of Science, Kasetsart University, Bangkok 10900, Thailand
[4] Department of Agronomy, Faculty of Agriculture, Kasetsart University, Bangkok 10900, Thailand; fagrtpc@ku.ac.th
[5] Omics Center for Agriculture, Bioresources, Food and Health, Kasetsart University, Bangkok 10900, Thailand
* Correspondence: fsciwcp@ku.ac.th (W.P.); fscipdj@ku.ac.th (P.J.)

Abstract: Alkaloids are a class of secondary metabolites that play multifaceted roles in plant physiology, including defense mechanisms and interactions with other organisms. The alkaloids from *Piper retrofractum* (Javanese long pepper) fruits offer potential alternatives to synthetic pesticides due to their natural origin and insecticide properties. However, information on particular alkaloid biosynthesis pathways is required to enhance individual alkaloid production via metabolic engineering. Here, we perform HPLC profiling to demonstrate that fruit ripening influences the alkaloid diversity in *P. retrofractum*. De novo transcriptomic profiling of young, green mature, and red ripened fruits revealed that the piperine biosynthesis pathway genes were highly upregulated in the mature fruits. However, an enhanced accumulation of methyl piperate and guineensine in the ripened fruit was observed, entailing ripening-related differential gene expression to synchronize the alkaloid biosyntheses. Gene expression clustering and functional enrichment analysis identified a large group of genes involved in diverse biosynthetic processes explicitly enriched in the ripened fruits. A cohort of genes encoding for "Alkaloid Biosynthesis", remarkably upregulated in the ripening fruits, indicates they may function directly in alkaloid diversity during a later stage of fruit development. This study provides the basis for metabolic engineering to enhance alkaloid diversity and production.

Keywords: alkaloid; differential gene expression; *Piper retrofractum*; piperine; RNA-seq; transcriptome

Citation: Meechuen, M.; Pimsawang, L.; Chaisan, T.; Samipak, S.; Pluempanupat, W.; Juntawong, P. Comparative Transcriptome Analysis Reveals Genes Associated with Alkaloid Diversity in Javanese Long Pepper (*Piper retrofractum*) Fruits. *Int. J. Plant Biol.* **2023**, *14*, 896–909. https://doi.org/10.3390/ijpb14040066

Academic Editor: Maurizio Cocucci

Received: 11 September 2023
Revised: 3 October 2023
Accepted: 3 October 2023
Published: 6 October 2023

1. Introduction

Plants are natural factories, producing diverse secondary metabolites, including alkaloids, terpenoids, and phenylpropanoids. These compounds exhibit a wide array of biological activities that have the potential to improve human health through applications in the pharmaceutical and food industries. The tradition of employing certain plants in traditional medicine finds ongoing validation as scientific investigation consistently confirms their effects [1].

Piper retrofractum, or Javanese long pepper, is a tropical plant from the Piperaceae family native to Southeast Asia. Many species of this family, such as *Piper nigrum* (black pepper), *Piper longum* (Indian long pepper), and *Piper methysticum* (kava kava), have been used in traditional medicine for centuries. *P. retrofractum* fruits are used as a spice in cooking and have been reported to contain a wide range of biological activities, including

antioxidant [2], anti-obesity activity [3], antifungal [4], antidiabetic [5], and antibacterial properties [6].

One significant problem resulting in major crop loss worldwide is insect infestation. The Food and Agriculture Organization (FAO) reported that insect pests cause between 20 and 40 percent loss of global crop production every year [7]. Synthetic chemical pesticides can be applied to increase the quality of crop production. However, the continuous use of these chemical pesticides resulted in environmental contamination. Moreover, it will become increasingly challenging to manage the infestation because of reduced effectiveness due to the development of pesticidal resistance from insect pests. Therefore, finding alternatives to chemical pesticides is an urgent concern. Interestingly, several pieces of evidence demonstrated insecticidal activity from *P. retrofractum* fruit extracted containing a piperic acid derivative, methyl piperate, and the alkaloids piperine, pipernonaline, and guineensine [8,9]. Therefore, unraveling the genes involved in the biosynthesis of these pesticide alternatives is required for large-scale production through metabolic engineering.

The maturation of fruits in medicinal herbs is a multifaceted process that demands a combination of physiological and morphological transformations and secondary metabolic activities [10]. Generally, biosynthesis of alkaloids starts from primary metabolites such as amino acids, organic acids, and sugars and is subsequently modified depending on cell types, developmental stages, and environmental signals [11]. In the case of fruit development, several lines of evidence suggest that alkaloid dynamics are related to this event [12–15]. Unfortunately, there is a lack of available genomic information, specific genes, and pathways involved in alkaloid diversity in *P. retrofractum*. However, a recent study on the effects of *P. retrofractum* fruit maturity on piperine, a major pungent alkaloid, suggested that the maturity stage significantly influenced the piperine content [16].

De novo transcriptome construction is typically conducted for gene discovery and metabolic pathway reconstitution in non-model organisms. Subsequently, comparative transcriptomic analysis can be employed to comprehensively understand how cells respond to specific conditions [17]. Our previous studies successfully applied this method to compare genome-wide gene expression in non-model organisms, including a microalga, *Scenedesmus acutus* [17] and a legume crop, *Vigna vexillata* [18]. Therefore, de novo transcriptome analysis and comparative transcriptome profiling could provide a basic understanding of the molecular responses related to alkaloid dynamics in *P. retrofractum*.

This study aims to identify the genes and pathways involved in alkaloid diversity from *P. retrofractum* fruits at different developmental stages using a combination of HPLC profiling, de novo transcriptome construction, and a comparative transcriptomic approach. This research has the potential to offer valuable insights into the genes and pathways responsible for the diversity of alkaloids in *P. retrofractum* fruits.

2. Materials and Methods

2.1. Plant Materials

The plant variety employed in this study was collected from Bueng Kan province, Thailand. While unpublished, our initial investigations indicated that this particular variety demonstrated the highest efficacy in terms of pesticide activity. In order to explore the potential connection between changes in alkaloid diversity and the advancement of fruit development, we gathered young, mature, and ripened *P. retrofractum* fruits from plants cultivated in outdoor soil at the National Corn and Sorghum Research Center in Nakhon Ratchasima, Thailand. Concurrently, we collected young leaves from these same plants for subsequent differential gene expression analysis.

2.2. HPLC Analysis

In this experiment, pooled samples (3–5 fruits) were used. The dried young, mature, and ripened fruits of *P. retrofractum* were ground into a powder. Approximately 300 mg of dried samples was extracted using maceration with hexane (1/10 w(g)/v(mL)) over seven days. All crude extracts were filtered using vacuum filtration with a Buchner funnel, and

the solvent was removed using a rotary evaporator (Heidolph, Germany) and stored at 4 °C in a refrigerator.

HPLC analysis was performed on Agilent 1200 series (Palo Alto, CA, USA) with UV-diode array detector and Ascentis C18 column (150 × 4.6 mm, 5 µm particle size). An aqueous solution containing 10 mM ammonium acetate (A) and MeOH (B) was used as the eluent. The following elution system was applied: from 20–90% B within 7 min, from 90–100% B within 11 min, 100% B was kept for 5 min, and from 100–20% B within 5 min with a flow rate of 1.0 mL/min. The injected concentration of the crude extracts was set to 10 mg/mL in pure methanol (MeOH), and an injection volume was 20 µL (containing 0.2 mg of the crude extract). The wavelength of detection was set at 230 nm. All samples were analyzed in triplicates. The peak at 10.08, 10.43, 13.29, and 16.04 min were identified as piperine, methyl piperate, pipernonaline, and guineensine, respectively, compared with the peak from each isolated compound [8].

2.3. RNA Extraction, Library Preparation, and Sequencing

Total RNA samples were extracted and treated with DNase using a GF-1 Total RNA Extraction Kit (Vivantis, Shah Alam, Malaysia) according to the manufacturer's protocol. Three replicates of total RNA samples were used for transcriptome analysis. The integrity of the RNA samples (RIN) was evaluated using an RNA 6000 Nano Kit on Agilent2100 Bioanalyzer (Agilent Technologies, Waldbronn, Germany). Samples with a RIN > 7 were used for library construction. Next, 3 µg of total RNAs was used to generate a sequencing library using an Illumina TruSeq Stranded mRNA LT Sample Prep Kit (Illumina, San Diego, CA, USA) following the manufacturer's instructions. Libraries were sequenced by an Illumina NovaSeq 6000 System according to the manufacturer's instructions. Sequencing was carried out using a 2 × 150 bp paired-end (PE) configuration. Quality control filtering and 3′ end trimming were analyzed using the FASTX-toolkit (http://hannonlab.cshl.edu/fastx_toolkit/index.html, released date 5 January 2014) and Trimmomatic software (version 0.36) [19].

2.4. De Novo Transcriptomic Assembly

FASTQ files were assembled using Trinity [20]. The longest open reading frames and amino acid sequences were obtained via Transdecoder [21]. The completeness of the assembled transcriptome was further analyzed by BUSCO [22].

2.5. Ortholog Identification

Orthologs among *P. retrofractum*, *P. nigrum*, and *A. thaliana* (TAIR10) were assigned by Orthovenn2 [23] using the default setting (e-value cut-off of 1×10^{-5} for all protein similarity comparison and inflation value for the generation of orthologous clusters of 1.5).

2.6. Differential Gene Expression Analysis

For *P. retrofractum*, FASTQ reads and the assembled transcriptome were used to generate read count data via SALMON [11]. For *P. nigrum*, FASTQ files were aligned to the *P. nigrum* reference genome using HISAT2 [24]. Subsequently, the sequence alignment (SAM) files were created and used to generate read count data via the HTseq library [25]. Differentially expressed genes were calculated using the edgeR program [26], with the GLM (generalized linear model) method using an FDR cut-off of <0.05. Significant DEGs were selected based on the FDR <0.0001 and were required to have at least one comparison with a log2 fold change > 1 or <−1.

2.7. Gene Ontology Enrichment Analysis

Gene ontology was assigned via GOMAP [27] using Linux command lines. Gene ontology enrichment analysis was performed using the GOHyperGAll function [28] in the R environment. Significant GO terms were filtered using an adjusted *p*-value of <0.05.

2.8. Cluster Analysis

Co-regulated genes were identified using fuzzy k-means clustering with Euclidean correlation for the distance measure, a membership exponent of 1.1, a maximal number of iterations of 5000, and 40 clusters [29]. The mean SLR value for each cluster was determined for summary visualization.

3. Results

3.1. Fruit Ripening Affects the Alkaloid Diversity

To test whether alkaloid diversity changes are related to fruit ripening, we collected *P. retrofractum* fruits at three developmental stages: young, mature, and ripened (Figure 1).

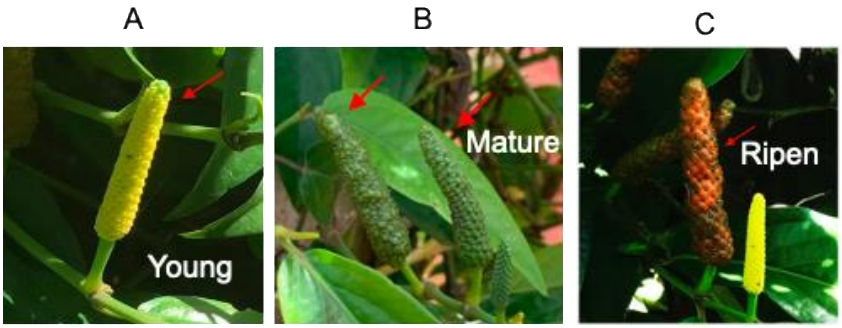

Figure 1. Javanese long paper fruits. Representative of (**A**) young, (**B**) mature, and (**C**) ripened fruits. Red arrows indicate particular developmental stages.

The dried young, mature, and ripened fruits of *P. retrofractum* were hexane extracted, since we previously showed that almost all hexane-isolated compounds were alkaloids except for methyl piperate [8]. Based on the HPLC profile compared to those isolated compounds (Figure 2A), our results demonstrated the dynamic of alkaloid diversity during fruit development. We focus on piperine, a major alkaloid found in the Piperaceae. Methyl piperate, pipernonaline, and guineensine were also evaluated due to their insecticidal activities [8]. Of these, quantitative analysis revealed that in young fruits, only pipernonaline could be found (Figure 2B). In mature and ripened fruits, piperine was the most abundant, followed by pipernonaline, guineensine, and methyl piperate, respectively, as indicated by the integrated peak area (Figure 2B). The comparison between the integrated peak area among the ripened and mature fruits revealed that methyl piperate and guineensine were 4.4- and 2.37-fold higher in the ripened fruit, respectively (Figure 2C). In contrast, the fold changes of piperine and pipernonaline comparing the ripened and mature fruits were lower (1.38 and 1.27-fold, respectively; Figure 2C). Together, these data indicate that fruit developmental stages strongly affect alkaloid diversity.

3.2. De Novo Transcriptome Construction from P. retrofractum Fruits and Leaves

RNA-seq data from young, mature, and ripened fruits and young leaves were used for de novo transcriptome construction. The transcriptome assembly yielded 181,299 genes consisting of 373,782 transcripts with an average transcript length of 1140.35 bp (N50 = 2091 bp) and GC content of 41.82% (Figure 3A; Supplementary File S1). Benchmarking Universal Single-Copy Ortholog (BUSCO) assessment revealed 97.65% (415/425 number of BUSCOs) completeness of the expected genes, 2.35% (10/425 number of BUSCOs) fragmented genes, and no missing genes (Figure 3B), suggesting the reliability of the assembled transcriptomic data.

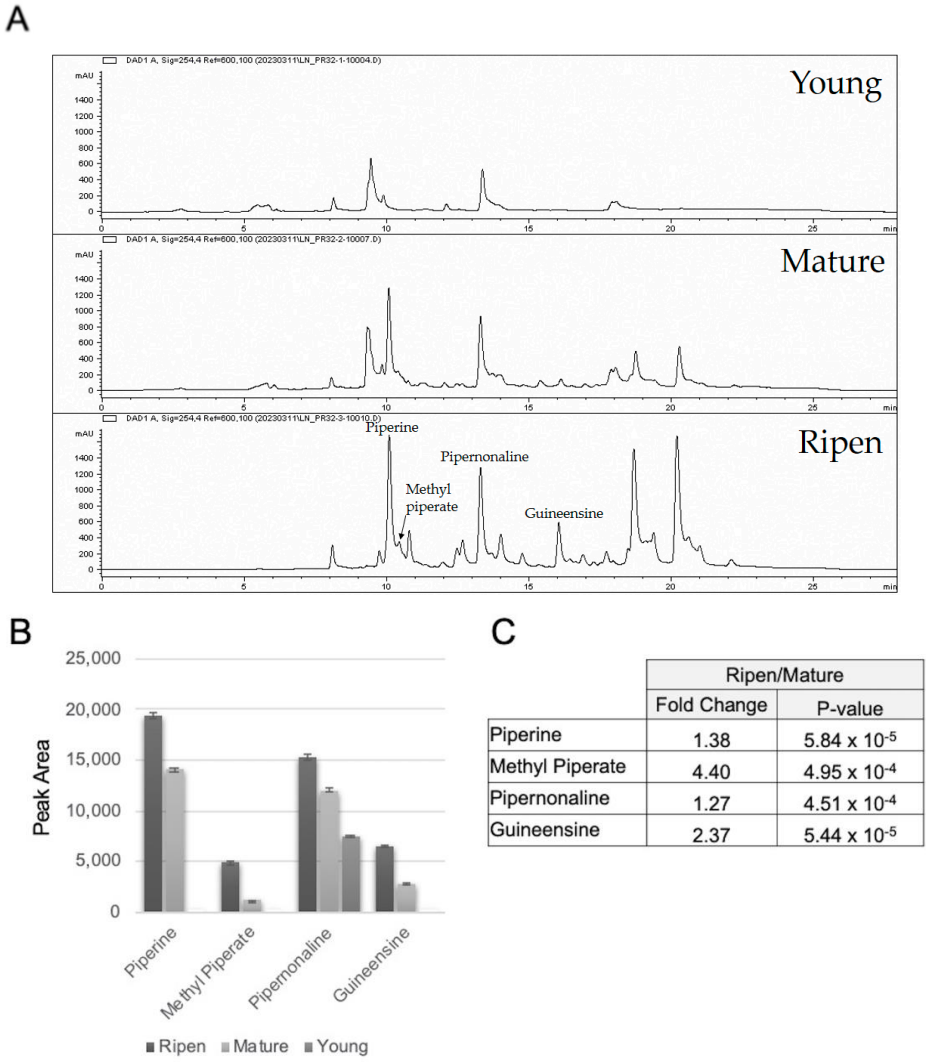

Figure 2. Composition and quantification of n-hexane extract from young, mature, and ripened *P. retrofractum* fruits. (**A**) Representative HPLC profiles. Conditions: column, reversed-phase Ascentis C18 (150 mm × 4.6 mm i.d., 5 µm); mobile phase, 10 mM aqueous ammonium acetate–methanol in gradient mode; flow rate, 1.0 mL/min; UV wavelength: 254 nm. (**B**) The quantitative peak area based on 0.2 mg of each extract on the flow rate separation shown in (**A**). Error bars represent standard deviation (n = 3). (**C**) Peak area comparison between ripened and mature fruits. p-values were calculated via t-test (n = 3).

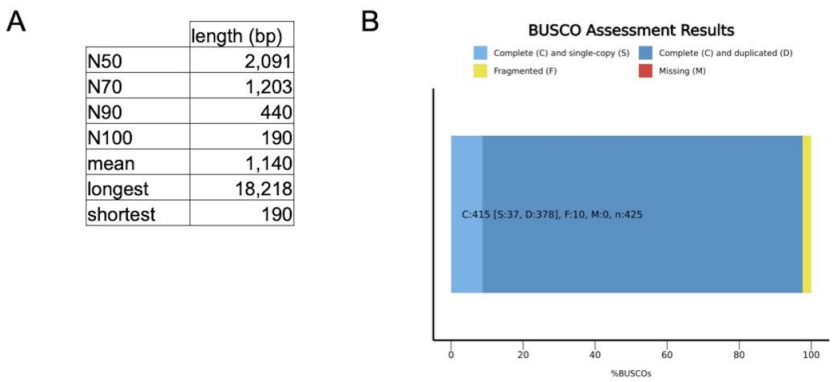

Figure 3. De novo transcriptome assembly evaluation. (**A**) Assembly statistics. (**B**) BUSCO assessment results from the Viridiplantae lineage dataset (number of BUSCOs: 425, number of genomes: 57).

To perform functional characterization of the assembled transcriptome, the candidate open reading frames (>100 amino acids; 198,548 protein-coding transcripts; Supplementary File S2) obtained by Transdecoder were annotated using BLASTP to the *Arabidopsis thaliana* proteins (TAIR10 version) and BlastKOALA [30] for KEGG Ortholog (KO) assignment and KEGG mapping (Table S1).

3.3. Transcriptomic Reprogramming during P. retrofractum Fruit Development

Three biological replicates of young, mature, and ripened fruit samples were included for differential gene expression analysis. Because a previous study involving black pepper demonstrated that the gene expression level of piperine and piperamide syntheses was nearly absent in young leaves [27], in this study, we contrasted the fruit transcriptome with leaf to identify genes highly expressed in fruits but not in leaves. SALMON was applied to generate highly accurate transcript-level quantification estimates from RNA-seq data [11]. The number of reads generated by SALMON was acquired for differential gene expression analysis using edgeR [26]. Differentially expressed genes (DEGs) from six comparisons were calculated: young/leaf, mature/leaf, ripen/leaf, mature/ripen, mature/young, and ripen/young. DEGs with significant changes in expression evaluated based on the false discovery rate (FDR) < 0.0001 were kept for further analysis (Table S2). Three out of six comparisons, young/leaf, mature/leaf, and ripen/leaf, were used to identify DEGs highly expressed in fruits but not in leaves. However, the other three comparisons, mature/ripen, mature/young, and ripen/young, were calculated to compare expression across the developmental stages.

The number of DEGs from young/leaf, mature/leaf, and ripen/leaf are 2232, 2556, and 7163, respectively (Figure 4A). The ripened fruits have approximately three times the number of DEGs, indicating that fruit ripening strongly affects physiological and molecular alterations.

To investigate the fruit developmental changes, GO enrichment analysis was performed on up- and downregulated DEGs from young/leaf, mature/leaf, and ripen/leaf comparisons (Table S3; Figure 4B). Interestingly, the "regulation of cellular macromolecule biosynthetic process" GO term was associated with the upregulated DEGs in all three fruit developmental stages (Figure 4B), whereas the "chlorophyll biosynthetic process" was commonly downregulated at all three stages (Figure 4C). Intriguingly, among the upregulated DEGs found only in mature/leaf ("232") and ripen/leaf ("2131") comparisons, subsets of DEGs involving in "secondary metabolic processes" were identified (Figure 4B,C) indicating the involvement of secondary metabolite biosynthesis during fruit development.

3.4. Cross-Species Transcriptomic Analyses Identified Piperine Biosynthesis Genes in P. retrofractum

To identify piperine biosynthetic genes in *P. retrofractum*, we began by assigning the ortholog clusters among the two Piperaceae species, *P. retrofractum* and *P. nigrum*. For the ortholog annotation purpose, the Arabidopsis representative genes were included (Figure 5A; Table S4). The piperine biosynthetic pathway and sequences of piperine biosynthetic genes were obtained from Schnabel et al. [31] (Figure 5B). We reanalyzed the *P. nigrum* fruit RNA-seq data [31] using the complete reference genome [32] to obtain the differential gene expression profiles (Table S5). The gene expression profiles were compared among the two species. Of the four enzymes [31,33,34], CYP719A37, piperamide synthase, and piperine synthase were upregulated in the *P. retrofractum* mature and ripened fruits (Figure 5C).

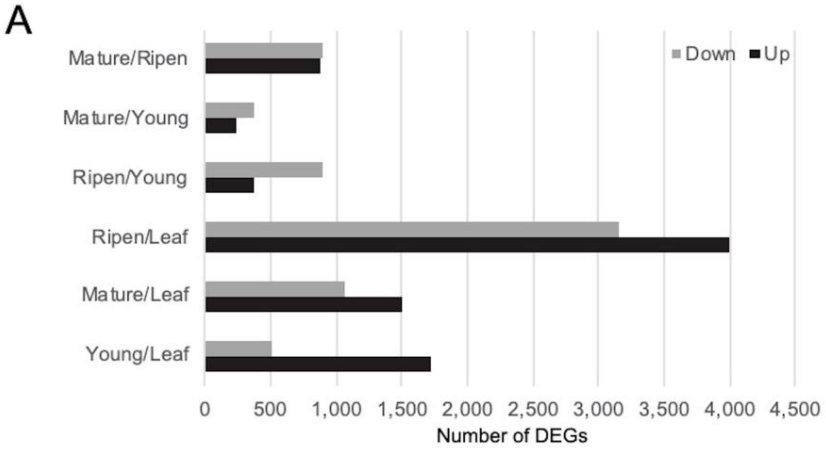

B

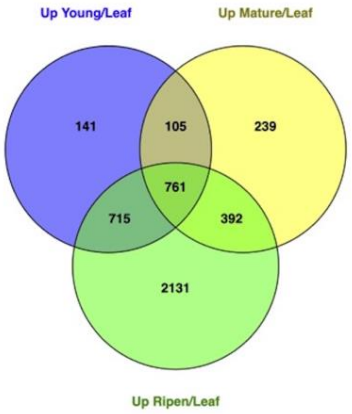

Cluster	Padj	Term
141	5.30×10^{-6}	response to hormone
141	1.52×10^{-3}	wax biosynthetic process
105	1.00×10^{-3}	proanthocyanidin biosynthetic process
105	1.94×10^{-3}	post-embryonic animal organ development
239	1.15×10^{-14}	secondary metabolic process
239	7.03×10^{-8}	green leaf volatile biosynthetic process
715	4.96×10^{-31}	response to chemical
715	1.40×10^{-11}	glycoside metabolic process
761	7.5×10^{-26}	regulation of cellular macromolecule biosynthetic process
761	1.66×10^{-25}	response to oxygen-containing compound
392	1.12×10^{-9}	response to oxidative stress
392	3.86×10^{-5}	epidermis morphogenesis
2131	1.76×10^{-87}	response to oxygen-containing compound
2131	1.11×10^{-40}	secondary metabolic process

C

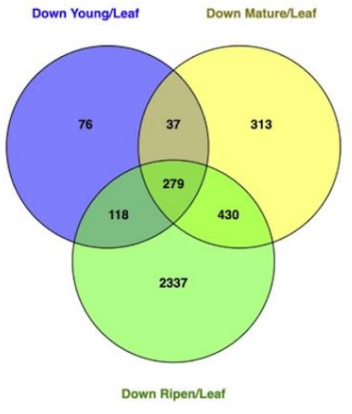

Cluster	Padj	Term
76	6.32×10^{-11}	response to copper ion
76	1.12×10^{-10}	response to ethanol
37	6.03×10^{-3}	steroid biosynthetic process
37	1.43×10^{-2}	lignin metabolic process
313	3.75×10^{-26}	cytoskeleton organization
313	2.84×10^{-16}	DNA-templated DNA replication
118	3.99×10^{-23}	photosynthesis
118	3.92×10^{-9}	carboxylic acid metabolic process
279	6.67×10^{-16}	shoot system morphogenesis
279	1.49×10^{-12}	chlorophyll biosynthetic process
430	1.93×10^{-17}	nucleosome assembly
430	1.76×10^{-15}	gibberellin biosynthetic process
2337	2.48×10^{-103}	photosynthesis
2337	2.48×10^{-43}	plastid organization

Figure 4. Differential gene expression during *P. retrofractum* fruit development. (**A**) The number of upregulated and downregulated differentially expressed genes (DEGs) from fruits of *P. retrofractum* under different developmental stages. (**B**) Upregulated and (**C**) downregulated DEGs and the top two enrichment biological process GO terms. Data used to generate this figure can be found in Tables S2 and S3.

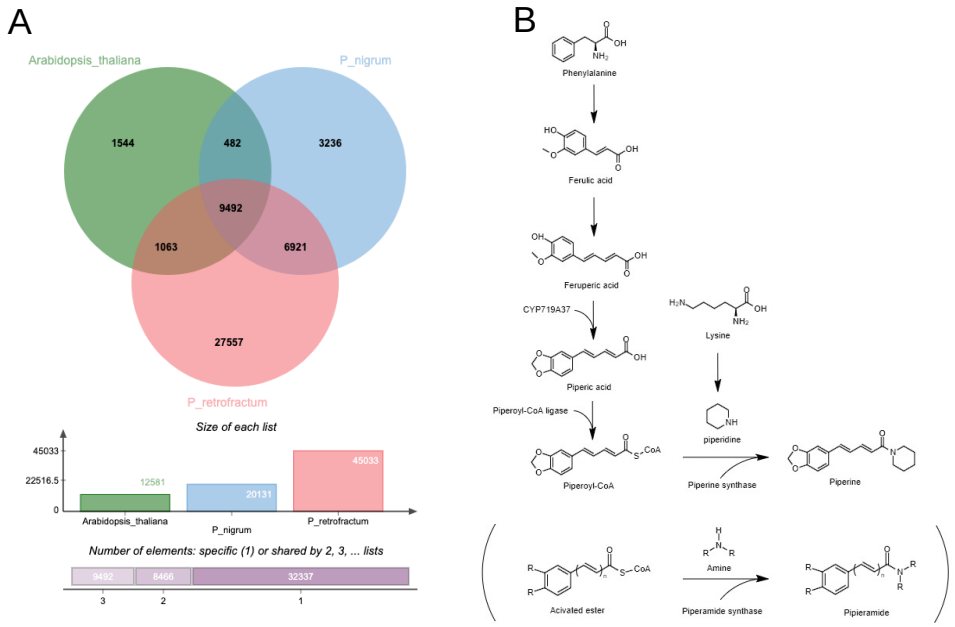

C

			P. retrofractum			*P. nigrum*	
Ortholog groups	**Species**	**ID**	**young/leaf**	**mature/leaf**	**ripen/leaf**	**d20/leaf**	**d40/leaf**
Piperine synthase	*P. retrofractum*	TRINITY_DN5015_c3_g1_i3	-1.33	7.36	4.56		
	P. retrofractum	TRINITY_DN5015_c3_g1_i2	0.77	10.76	8.19		
	P. nigrum	Pn11.2248				-1.48	3.49
	P. nigrum	Pn11.2279				-1.62	3.21
	P. nigrum	Pn12.1813				-1.54	2.71
Piperamide synthase	*P. nigrum*	Pn6.2477				-1.70	4.30
	P. retrofractum	TRINITY_DN12595_c1_g1_i1	-2.72	5.16	1.77		
	P. retrofractum	TRINITY_DN12595_c1_g1_i2	NA	NA	NA		
	P. retrofractum	TRINITY_DN12595_c1_g1_i3	-2.80	5.91	2.23		
CYP719A37	*P. retrofractum*	TRINITY_DN16025_c0_g1_i8	5.36	15.70	12.88		
	P. nigrum	Pn3.4770				-1.79	5.42
Piperic coenzyme A ligase	*P. retrofractum*	TRINITY_DN2482_c1_g1_i3	NA	NA	NA		
	P. retrofractum	TRINITY_DN2482_c1_g1_i13	NA	NA	NA		
	P. retrofractum	TRINITY_DN2482_c1_g1_i5	NA	NA	NA		
	P. nigrum	Pn24.611				NA	NA
	P. nigrum	Pn24.641				0.05	1.47
	P. nigrum	Pn24.640				-0.17	1.66
	P. nigrum	Pn24.638				NA	NA
	P. nigrum	Pn24.610				NA	NA

Figure 5. Identification of piperine and piperamide biosynthesis genes from *P. retrofractum* transcriptome. (**A**) Ortholog identification among *A. thaliana*, *P. nigrum*, and *P. retrofractum*. (**B**) Piperine and piperamide-related genes and their functions. (**C**) Comparison of the piperine and piperamide biosynthesis gene expression data from this study (*P. retrofractum*) and black pepper (*P. nigrum*). Data used to generate this figure can be found in Tables S2, S4 and S6. Yellow indicates upregulation, while blue represents downregulation.

Similarly, in *P. nigrum*, their expressions were upregulated in the day (d) 40 fruits but downregulated in d20 fruits (Figure 5C). Remarkably, in *P. retrofractum*, the expression of CYP719A37, piperamide synthase, and piperine synthase was more upregulated in the mature fruits compared to ripened fruits. As previously mentioned, HPLC profiling demonstrated relatively small changes in piperine accumulation when comparing mature and ripened fruits (Figure 1C). Presuming that transcript accumulation led to the biosynthetic product formation, our results indicate that in *P. retrofractum* fruit, the biosynthesis of piperine occurs predominantly in the mature stage.

3.5. A Group of Non-Piperine Alkaloid Biosynthesis DEGs was Explicitly Upregulated in the Ripened Fruits

Since the coexpression of genes can be leveraged to build the gene expression network, we applied fuzzy k-mean clustering analysis to identify genes that control *P. retrofractum* fruit alkaloid diversity (Figure 6A). The fuzzy algorithm is classified as a soft clustering

approach, which permits DEGs to be assigned to multiple clusters simultaneously. Consequently, it becomes valuable for identifying genes influenced by numerous factors and those that might encode a protein with more than one function. Our analysis included all six DEG comparisons and the number of clusters and membership exponent was determined through iterative experimentation. Ultimately, a total of 40 clusters was obtained as the final outcome. Subsequently, GO enrichment analysis was conducted to reveal the enriched functions (Table S6).

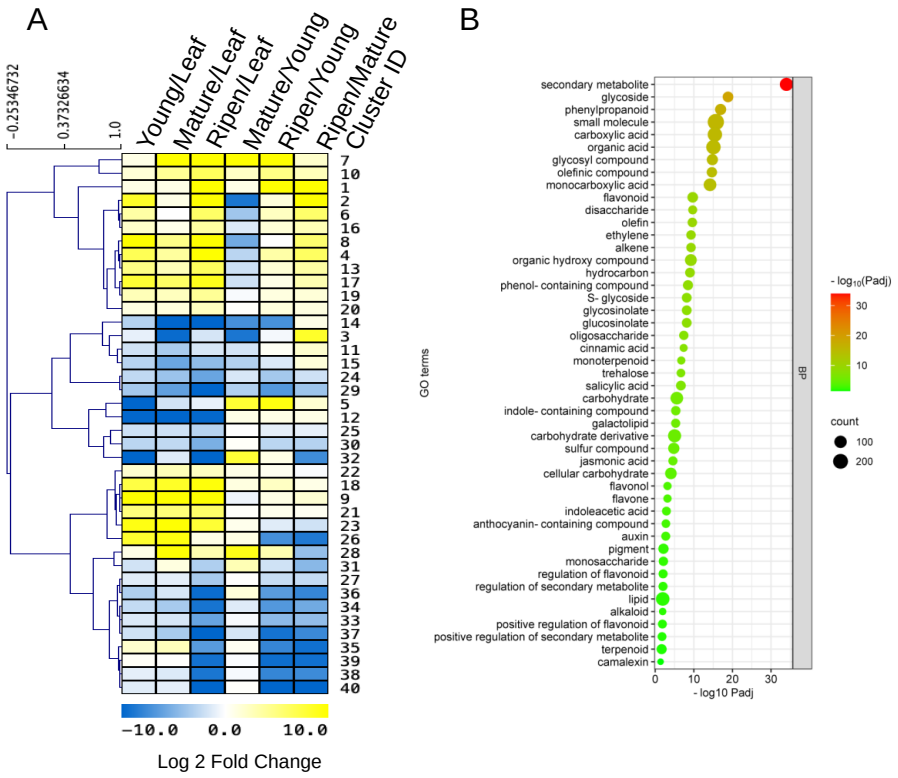

C

ID	Cluster ID	ATH best blast	Description	young/leaf	mature/leaf	ripen/ leaf	mature/young	ripen/young	ripen/mature	KO	EC-number	KO definition
TRINITY_DN16025_c0_g1_i2	2	AT4G13770	cytochrome P450, family 83, subfamily A, polypeptide 1	10.30	0.00	8.91	-10.30	-1.39	8.91			
TRINITY_DN10318_c0_g1_i1	4	AT5G07990	CYP75B1, CYTOCHROME P450 75B1, D501, TRANSPARENT TESTA 7, TT7	7.17	5.49	10.10	-1.68	2.93	4.61			
TRINITY_DN212_c2_g1_i1	4	AT3G03480	acetyl CoA:(Z)-3-hexen-1-ol acetyltransferase	4.96	1.69	11.36	-3.27	6.40	9.67	K19861	[EC:2.3.1.196 ,EC:2.3.1.232]	benzyl alcohol O-benzoyltransferase
TRINITY_DN274_c0_g1_i9	4	AT3G18370	C2 domain-containing protein	8.15	5.19	12.01	-2.96	3.86	6.82	K22374	[EC:1.1.1.285]	3''-deamino-3''-oxonicotianamine reductase
TRINITY_DN10885_c0_g1_i1	6	AT5G17540	HXXXD-type acyl-transferase family protein	3.89	1.21	6.85	-2.68	2.95	5.63	K19861	[EC:2.3.1.196 ,EC:2.3.1.232]	benzyl alcohol O-benzoyltransferase
TRINITY_DN42814_c0_g1_i3	6	AT2G45550	cytochrome P450, family 76, subfamily C, polypeptide 4	3.60	-2.11	5.20	-5.72	1.59	7.31			
TRINITY_DN16176_c0_g1_i2	13	AT5G54160	O-methyltransferase 1	2.81	1.76	6.29	-1.05	3.48	4.53			
TRINITY_DN7629_c0_g1_i16	13	AT4G35160	O-methyltransferase family protein	4.83	3.38	8.37	-1.45	3.54	4.99			
TRINITY_DN7058_c0_g1_i18	16	AT1G60710	NAD(P)-linked oxidoreductase superfamily protein	2.27	-0.06	3.48	-2.32	1.21	3.53	K05275	[EC:1.1.1.65]	pyridoxine 4-dehydrogenase
TRINITY_DN7115_c0_g1_i1	17	AT5G44390	FAD-binding Berberine family protein	7.01	4.93	8.42	-2.08	1.41	3.49			
TRINITY_DN14676_c0_g1_i2	19	AT2G45550	cytochrome P450, family 76, subfamily C, polypeptide 4	2.45	2.18	5.36	-0.27	2.91	3.18			

Figure 6. Coexpression and functional enrichment analysis of DEGs from *P. retrofractum* fruits. (**A**) Fuzzy kmean clustering. (**B**) Enriched "Biosynthetic Process" GO terms by combining DEGs from clusters 2, 4, 6, 8, 13, 16, 17, and 19. (**C**) Candidate transcripts enriched in the ripened fruits with roles in alkaloid biosynthesis/metabolism. Data used to generate this figure can be found in Tables S2 and S7. Yellow indicates upregulation, while blue represents downregulation.

We selected some clusters to describe here. Cluster 28 DEGs were highly expressed in mature and ripened fruits, but their expression was higher in the mature fruits enriched with the "alkaloid biosynthetic process" (Figure 6A; Table S6). Cluster 28 DEGs include piperine and piperamide synthases and CYP719A37 (Table S6). Thus, this cluster is representative of mature enriched piperine biosynthesis genes. Next, clusters 25, 27, 28, 30, 33, 36, 37, and 38 enriched with chloroplast-related GO terms were downregulated in fruits, especially in the mature and ripened stages (Figure 6A; Table S6). Clusters 13 and 16, associated with the "ethylene biosynthetic process", and cluster 6, associated with "respiratory burst", were upregulated in fruit, especially at the ripening stage (Figure 6A; Table S6).

We focused on a cohort of DEGs from clusters 2, 4, 6, 8, 13, 16, 17, and 19. These clusters are upregulated in fruits, indicating their roles in fruit development. However, comparing the developmental stages, we found that their abundance appeared generally higher in ripened fruits (Figure 6A). GO enrichment analysis reveals their function related to multiple "Biosynthetic Process" GO terms, indicating that these DEGs are involved in fruit-ripened metabolite production (Figure 6B; Table S7). Remarkably, DEGs related to the "alkaloid biosynthetic process" were enriched in these clusters. These alkaloid biosynthetic genes were non-piperine-related and included the benzyl alcohol O-benzoyltransferases, 3′-deamino-3′-oxonicotianamine reductase, pyridoxine 4-dehydrogenase, O-methyltransferase, and cytochrome P450 (Figure 6C).

4. Discussion

Alkaloid diversity undergoes significant variations during fruit development, contingent upon the plant species and the particular alkaloids present. Changes in alkaloid diversity at different stages of fruit development have been reported in several plant species; for example, chili (*Capsicum chinense*) [15], hawthorn (*Crataegus pinnatifida* var. major) [12], and tomato (*Solanum lycopersicum*) [13,14]. This study constructed de novo transcriptome and differential gene expression analysis to compare the gene expression profiles of *P. retrofractum* fruits at different developmental stages (Figure 1).

Our results established that fruit developmental stages could affect the dynamic of alkaloid diversity (Figure 2). A major alkaloid, piperine, had the highest abundance in ripened fruits (Figure 2B). The piperine level in the ripened fruit was slightly higher than in the mature fruits (Figure 2C). A study by Takahashi et al. [16] measuring the piperine level in *P. retrofractum* fruits at the green, orange, and red maturity stages found that the level was almost two times higher in the green maturing stage compared to the red maturity stage. Therefore, Takahashi's data similarly suggested that piperine accumulation mainly occurred in the green maturing fruits. The observed variations in piperine contents in the red ripened fruits in this study and Takahashi's study could be attributed to differences in cultivars, extraction/detection methods, and regional disparities. To support our hypothesis, the piperine content exhibited variations ranging from 2.75% to 0.022%, as determined by HPLC analysis across 24 distinct black pepper genotypes gathered from various locations across India [35]. Additionally, Schnabel et al. [27] conducted a time course of piperine accumulation in *P. nigrum* fruits and found no significant increase during the later stages of fruit development. Together, these findings suggest that piperine biosynthesis primarily occurs at the mature stages and demonstrate that the mechanism of piperine biosynthesis may be conserved among the Piperaceae family.

Regarding the quality of our *P. retrofractum* transcriptome, Trinity statistics and BUSCO assessments revealed that the assembled transcriptome could be used as a reference transcriptome for gene identification (Figure 3). However, a high number of complete and duplicated transcripts indicated that several isoforms of the same gene are included in the assembled transcriptome (Figure 3B). On average, over four transcript isoforms were reported per expressed gene in the plant model Arabidopsis [36]. These isoforms may be caused by alternative splicing, alternative transcription initiation sites, and alternative transcription termination sites.

Fruit maturing and ripening resulted in fruit transcriptomic reprogramming (Figure 4). The number of DEGs was almost three times higher in ripen/leaf compared to mature/leaf and young/leaf, indicating a significant transcriptome adjustment at the ripening stage (Figure 4A). The upregulation of the secondary metabolic process was explicitly observed in mature/leaf (Padj 1.15×10^{-14}) and ripen/leaf (Padj 1.11×10^{-40}) comparisons (Figure 3B). Since these two groups of DEGs do not overlap, these findings indicate that distinct processes contributed to the secondary metabolite accumulation in mature and ripened fruits. The commonly downregulated DEGs found in all stages of fruits are involved in the chlorophyll biosynthetic process (Figure 4C), similar to the results observed in the *P. nigrum* fruits [31].

Piperaceae exhibit a distinctive trait in their ability to biosynthesize significant quantities of piperine. Based on our results, we successfully identified key genes contributing to piperine biosynthesis by integrating the previously characterized *P. nigrum* genome information [32] and the *P. nigrum* fruit transcriptome data [31] (Figure 5). Interestingly, the expression of these key piperine biosynthetic genes was more robustly induced in mature fruits than in ripened fruits (Figure 5C). These findings support our idea that piperine biosynthesis in *P. retrofractum* fruits predominantly occurs in the mature stage. It should be noted that mRNA and metabolite accumulation, while linked through their roles in gene expression and metabolism, serve unique roles in cellular biology. In our study, the accumulation of piperine biosynthetic mRNAs reflects both gene transcriptional activity and mRNA decay rates. In contrast, piperine accumulation provides a direct and dynamic snapshot of cellular metabolic status.

Our results demonstrated that several biological processes contributed to the ripening of *P. retrofractum fruits*. Fruits are typically categorized into two physiological groups, climacteric and non-climacteric, based on their respiratory activity and the ethylene biosynthesis profiles accompanying the ripening process [37]. Our results revealed the enrichment of the ethylene biosynthetic process and respiratory burst in DEGs from the ripen-specific clusters (Tables S6 and S7). These findings strongly indicate that *P. retrofractum* fruits exhibit characteristics consistent with a climacteric nature, where ethylene biosynthesis and respiratory burst are essential for fruit ripening.

Prior investigations across various plant species have indicated that the level of fruit maturity may influence the synthesis of secondary metabolites [12–15]. Likewise, our findings suggest that secondary metabolites were the most prominently enriched among the various biosynthetic processes, mainly occurring in ripened fruits (Figure 6B).

Our study identified a cohort of non-piperine alkaloid biosynthesis DEGs particularly associated with the *P. retrofractum* ripened fruits (Figure 6B,C). Of these, the benzyl alcohol O-benzoyltransferases (BEBTs) represent a subset of the BAHD acyltransferase family. The BAHD acyltransferases play a significant role in catalyzing acyl transfer reactions involving alcohol and acyl-CoA substrates. Notably, BAHD acyltransferases can exhibit remarkable versatility in accepting different substrates, leading to the synthesis of a diverse array of compounds [38]. Evidently, in *P. nigrum*, among the two BAHD-like enzymes, piperine and piperamide synthases, which catalyze the formation of piperine and piperamides, the piperamide synthase exhibits greater substrate promiscuity than piperine synthase, as it can accommodate various precursor molecules and catalyze their conversion into multiple alkaloids [31].

Our results also recognized cytochrome P450 enzymes as a prominent factor influencing alkaloid diversity. Cytochrome P450 catalyzes a wide range of oxidative reactions, including hydroxylation, epoxidation, dealkylation, and ring-cleavage reactions, essential to forming structurally diverse alkaloids [39]. In addition, we identified three DEGs associated with extensive alkaloid diversity. First, 3′-deamino-3′-oxonicotianamine reductase participates in the biosynthesis of alkaloids like nicotine [40]. Second, pyridoxine 4-dehydrogenase relates to the biosynthesis of pyridoxine alkaloids [41]. Lastly, O-methyltransferases deliver methyl groups to precursor molecules in alkaloid biosynthesis [42].

We expect the basic knowledge obtained from this study will help enhance our understanding of the process related to alkaloid diversity and benefit alkaloid production via metabolic engineering in the future.

Supplementary Materials: The following supporting information can be downloaded at: https://www.mdpi.com/article/10.3390/ijpb14040066/s1, Supplementary File S1: De novo assembled transcriptome; Supplementary File S2: Polypeptide sequences; Table S1: Protein identification; Table S2: Differentially expressed genes; Table S3: Gene ontology enrichment analysis of differentially expressed genes; Table S4: Ortholog identification; Table S5: Differentially expressed genes of *P. nigrum* fruits; Table S6: Gene ontology enrichment analysis of clustered differentially expressed genes; Table S7: Gene ontology enrichment analysis of differentially expressed genes from clusters 2, 4, 6, 8, 13, 16, 17, and 19.

Author Contributions: Conceptualization, T.C., S.S., W.P. and P.J.; Methodology, W.P. and P.J.; Formal Analysis, M.M. and P.J.; Investigation, M.M. and L.P.; Resources, T.C.; Writing—Original Draft Preparation, P.J.; Writing—Review and Editing, P.J.; Visualization, M.M.; Supervision, W.P. and P.J.; Project Administration, P.J.; Funding Acquisition, W.P. and P.J. All authors have read and agreed to the published version of the manuscript.

Funding: This work was funded by the Agricultural Research Development Agency (Thailand; PRP6405031780), the Center of Excellence for Innovation in Chemistry (PERCH-CIC), the Ministry of Higher Education, Science, Research and Innovation (Thailand), and the Graduate School Fellowship Program from Kasetsart University.

Institutional Review Board Statement: Not applicable.

Informed Consent Statement: Not applicable.

Data Availability Statement: The datasets generated from the current study are available in the NCBI SRA database under the BioProject accession: PRJNA1006448.

Acknowledgments: We thank Jaruwan Sreeratree, Oratai Thakom, and Pimprapai Butsayaworapat for their technical assistance.

Conflicts of Interest: The authors declare no conflict of interest.

References

1. Salehi, B.; Zakaria, Z.A.; Gyawali, R.; Ibrahim, S.A.; Rajkovic, J.; Shinwari, Z.K.; Khan, T.; Sharifi-Rad, J.; Ozleyen, A.; Turkdonmez, E.; et al. Piper Species: A Comprehensive Review on Their Phytochemistry, Biological Activities and Applications. *Molecules* **2019**, *24*, 1364. [CrossRef] [PubMed]
2. Jadid, N.; Hidayati, D.; Hartanti, S.R.; Arraniry, B.A.; Rachman, R.Y.; Wikanta, W. Antioxidant activities of different solvent extracts of *Piper retrofractum* Vahl. using DPPH assay. In Proceedings of the Biodiversity and Biotechnology for Human Welfare, Surabaya, Indonesia, 15 October 2016; p. 020019.
3. Muharini, R.; Liu, Z.; Lin, W.; Proksch, P. New amides from the fruits of *Piper retrofractum*. *Tetrahedron Lett.* **2015**, *56*, 2521–2525. [CrossRef]
4. Luyen, B.T.T.; Tai, B.H.; Thao, N.P.; Yang, S.Y.; Cuong, N.M.; Kwon, Y.I.; Jang, H.D.; Kim, Y.H. A new phenylpropanoid and an alkylglycoside from *Piper retrofractum* leaves with their antioxidant and α-glucosidase inhibitory activity. *Bioorganic Med. Chem. Lett.* **2014**, *24*, 4120–4124. [CrossRef]
5. Kim, K.J.; Lee, M.-S.; Jo, K.; Hwang, J.-K. Piperidine alkaloids from *Piper retrofractum* Vahl. protect against high-fat diet-induced obesity by regulating lipid metabolism and activating AMP-activated protein kinase. *Biochem. Biophys. Res. Commun.* **2011**, *411*, 219–225. [CrossRef]
6. Tewtrakul, S.; Hase, K.; Kadota, S.; Namba, T.; Komatsu, K.; Tanaka, K. Fruit Oil Composition of *Piper chaba* Hunt., *P. longum* L. and *P. nigrum* L. *J. Essent. Oil Res.* **2000**, *12*, 603–608. [CrossRef]
7. FAO. New Standards to Curb the Global Spread of Plant Pests and Diseases. Available online: https://www.fao.org/news/story/en/item/1187738/icode/ (accessed on 10 August 2023).
8. Ratwatthananon, A.; Yooboon, T.; Bullangpoti, V.; Pluempanupat, W. Insecticidal activity of *Piper retrofractum* fruit extracts and isolated compounds against *Spodoptera litura*. *Agric. Nat. Resour.* **2020**, *54*, 447–452. [CrossRef]
9. Park, B.-S.; Lee, S.-E.; Choi, W.-S.; Jeong, C.-Y.; Song, C.; Cho, K.-Y. Insecticidal and acaricidal activity of pipernonaline and piperoctadecalidine derived from dried fruits of *Piper longum* L. *Crop Prot.* **2002**, *21*, 249–251. [CrossRef]
10. Li, Y.; Kong, D.; Fu, Y.; Sussman, M.R.; Wu, H. The effect of developmental and environmental factors on secondary metabolites in medicinal plants. *Plant Physiol. Biochem.* **2020**, *148*, 80–89. [CrossRef]

11. Patro, R.; Duggal, G.; Love, M.I.; Irizarry, R.A.; Kingsford, C. Salmon provides fast and bias-aware quantification of transcript expression. *Nat. Methods* **2017**, *14*, 417–419. [CrossRef]
12. Wang, Y.; Hao, R.; Guo, R.; Nong, H.; Qin, Y.; Dong, N. Integrative Analysis of Metabolome and Transcriptome Reveals Molecular Insight into Metabolomic Variations during Hawthorn Fruit Development. *Metabolites* **2023**, *13*, 423. [CrossRef]
13. Ngo, T.H.; Park, J.; Jo, Y.D.; Jin, C.H.; Jung, C.-H.; Nam, B.; Han, A.-R.; Nam, J.-W. Content of Two Major Steroidal Glycoalkaloids in Tomato (*Solanum lycopersicum* cv. Micro-Tom) Mutant Lines at Different Ripening Stages. *Plants* **2022**, *11*, 2895. [CrossRef] [PubMed]
14. Yang, X.; Zhao, X.; Fu, D.; Zhao, Y. Integrated Analysis of Widely Targeted Metabolomics and Transcriptomics Reveals the Effects of Transcription Factor NOR-like1 on Alkaloids, Phenolic Acids, and Flavonoids in Tomato at Different Ripening Stages. *Metabolites* **2022**, *12*, 1296. [CrossRef] [PubMed]
15. Rodrigues-Salvador, A.; Lana-Costa, J.; Omena-Garcia, R.P.; Batista-Silva, W.; Scossa, F.; Rosado-Souza, L.; Perez-Diaz, J.L.; Menezes-Silva, P.E.; DaMatta, F.M.; Sulpice, R.; et al. Metabolic shifts during fruit development in pungent and non-pungent peppers. *Food Chem.* **2022**, *375*, 131850. [CrossRef] [PubMed]
16. Takahashi, M.; Hirose, N.; Ohno, S.; Arakaki, M.; Wada, K. Flavor characteristics and antioxidant capacities of hihatsumodoki (*Piper retrofractum* Vahl) fresh fruit at three edible maturity stages. *J. Food Sci. Technol.* **2018**, *55*, 1295–1305. [CrossRef]
17. Sirikhachornkit, A.; Suttangkakul, A.; Vuttipongchaikij, S.; Juntawong, P. De novo transcriptome analysis and gene expression profiling of an oleaginous microalga Scenedesmus acutus TISTR8540 during nitrogen deprivation-induced lipid accumulation. *Sci. Rep.* **2018**, *8*, 3668. [CrossRef]
18. Butsayawarapat, P.; Juntawong, P.; Khamsuk, O.; Somta, P. Comparative Transcriptome Analysis of Waterlogging-Sensitive and Tolerant Zombi Pea (*Vigna vexillata*) Reveals Energy Conservation and Root Plasticity Controlling Waterlogging Tolerance. *Plants* **2019**, *8*, 264. [CrossRef]
19. Bolger, A.M.; Lohse, M.; Usadel, B. Trimmomatic: A flexible trimmer for Illumina sequence data. *Bioinformatics* **2014**, *30*, 2114–2120. [CrossRef]
20. Grabherr, M.G.; Haas, B.J.; Yassour, M.; Levin, J.Z.; Thompson, D.A.; Amit, I.; Adiconis, X.; Fan, L.; Raychowdhury, R.; Zeng, Q.; et al. Full-length transcriptome assembly from RNA-Seq data without a reference genome. *Nat. Biotechnol.* **2011**, *29*, 644–652. [CrossRef]
21. Haas, B.J.; Papanicolaou, A.; Yassour, M.; Grabherr, M.; Blood, P.D.; Bowden, J.; Couger, M.B.; Eccles, D.; Li, B.; Lieber, M.; et al. De novo transcript sequence reconstruction from RNA-seq using the Trinity platform for reference generation and analysis. *Nat. Protoc.* **2013**, *8*, 1494–1512. [CrossRef]
22. Simão, F.A.; Waterhouse, R.M.; Ioannidis, P.; Kriventseva, E.V.; Zdobnov, E.M. BUSCO: Assessing genome assembly and annotation completeness with single-copy orthologs. *Bioinformatics* **2015**, *31*, 3210–3212. [CrossRef]
23. Xu, L.; Dong, Z.; Fang, L.; Luo, Y.; Wei, Z.; Guo, H.; Zhang, G.; Gu, Y.Q.; Coleman-Derr, D.; Xia, Q.; et al. OrthoVenn2: A web server for whole-genome comparison and annotation of orthologous clusters across multiple species. *Nucleic Acids Res.* **2019**, *47*, W52–W58. [CrossRef] [PubMed]
24. Kim, D.; Paggi, J.M.; Park, C.; Bennett, C.; Salzberg, S.L. Graph-based genome alignment and genotyping with HISAT2 and HISAT-genotype. *Nat. Biotechnol.* **2019**, *37*, 907–915. [CrossRef] [PubMed]
25. Putri, G.H.; Anders, S.; Pyl, P.T.; Pimanda, J.E.; Zanini, F. Analysing high-throughput sequencing data in Python with HTSeq 2.0. *Bioinformatics* **2022**, *38*, 2943–2945. [CrossRef] [PubMed]
26. Robinson, M.D.; McCarthy, D.J.; Smyth, G.K. edgeR: A Bioconductor package for differential expression analysis of digital gene expression data. *Bioinformatics* **2009**, *26*, 139–140. [CrossRef]
27. Wimalanathan, K.; Lawrence-Dill, C.J. Gene Ontology Meta Annotator for Plants (GOMAP). *Plant Methods* **2021**, *17*, 54. [CrossRef]
28. Horan, K.; Jang, C.; Bailey-Serres, J.; Mittler, R.; Shelton, C.; Harper, J.F.; Zhu, J.-K.; Cushman, J.C.; Gollery, M.; Girke, T. Annotating Genes of Known and Unknown Function by Large-Scale Coexpression Analysis. *Plant Physiol.* **2008**, *147*, 41–57. [CrossRef]
29. Sreeratree, J.; Butsayawarapat, P.; Chaisan, T.; Somta, P.; Juntawong, P. RNA-Seq Reveals Waterlogging-Triggered Root Plasticity in Mungbean Associated with Ethylene and Jasmonic Acid Signal Integrators for Root Regeneration. *Plants* **2022**, *11*, 930. [CrossRef]
30. Kanehisa, M.; Sato, Y.; Morishima, K. BlastKOALA and GhostKOALA: KEGG Tools for Functional Characterization of Genome and Metagenome Sequences. *J. Mol. Biol.* **2016**, *428*, 726–731. [CrossRef]
31. Schnabel, A.; Athmer, B.; Manke, K.; Schumacher, F.; Cotinguiba, F.; Vogt, T. Identification and characterization of piperine synthase from black pepper, *Piper nigrum* L. *Commun. Biol.* **2021**, *4*, 445. [CrossRef]
32. Hu, L.; Xu, Z.; Wang, M.; Fan, R.; Yuan, D.; Wu, B.; Wu, H.; Qin, X.; Yan, L.; Tan, L.; et al. The chromosome-scale reference genome of black pepper provides insight into piperine biosynthesis. *Nat. Commun.* **2019**, *10*, 4702. [CrossRef]
33. Schnabel, A.; Cotinguiba, F.; Athmer, B.; Yang, C.; Westermann, B.; Schaks, A.; Porzel, A.; Brandt, W.; Schumacher, F.; Vogt, T. A piperic acid CoA ligase produces a putative precursor of piperine, the pungent principle from black pepper fruits. *Plant J.* **2020**, *102*, 569–581. [CrossRef]
34. Schnabel, A.; Cotinguiba, F.; Athmer, B.; Vogt, T. Piper nigrum CYP719A37 Catalyzes the Decisive Methylenedioxy Bridge Formation in Piperine Biosynthesis. *Plants* **2021**, *10*, 128. [CrossRef] [PubMed]
35. Gurung, K.; Manivannan, S. Morphological characterization and secondary metabolites profile of black pepper (*Piper nigrum* L.) genotypes from Sikkim. *J. Spices Aromat. Crops* **2020**, *29*, 98–104. [CrossRef]

36. Thomas, Q.A.; Ard, R.; Liu, J.; Li, B.; Wang, J.; Pelechano, V.; Marquardt, S. Transcript isoform sequencing reveals widespread promoter-proximal transcriptional termination in Arabidopsis. *Nat. Commun.* **2020**, *11*, 2589. [CrossRef] [PubMed]
37. Osorio, S.; Scossa, F.; Fernie, A. Molecular regulation of fruit ripening. *Front. Plant Sci.* **2013**, *4*, 198. [CrossRef]
38. Moghe, G.; Kruse, L.H.; Petersen, M.; Scossa, F.; Fernie, A.R.; Gaquerel, E.; D'Auria, J.C. BAHD Company: The Ever-Expanding Roles of the BAHD Acyltransferase Gene Family in Plants. *Annu. Rev. Plant Biol.* **2023**, *74*, 165–194. [CrossRef]
39. Chakraborty, P.; Biswas, A.; Dey, S.; Bhattacharjee, T.; Chakrabarty, S. Cytochrome P450 Gene Families: Role in Plant Secondary Metabolites Production and Plant Defense. *J. Xenobiot.* **2023**, *13*, 402–423. [CrossRef]
40. Shojima, S.; Nishizawa, N.-K.; Fushiya, S.; Nozoe, S.; Irifune, T.; Mori, S. Biosynthesis of phytosiderophores. In vitro biosynthesis of 2′-deoxymugineic acid from l-methionine and nicotianamine. *Plant Physiol.* **1990**, *93*, 1497–1503. [CrossRef]
41. Holzer, H.; Schneider, S. Reinigung und charakterisierung einer TPN-abhängigen pyridoxol-dehydrogenase aus bierhefe. *Biochim. Biophys. Acta* **1961**, *48*, 71–76. [CrossRef]
42. Morishige, T.; Tamakoshi, M.; Takemura, T.; Sato, F. Molecular characterization of O-methyltransferases involved in isoquinoline alkaloid biosynthesis in *Coptis japonica*. *Proc. Jpn. Acad. Ser. B* **2010**, *86*, 757–768. [CrossRef]